Electron Ionization Mass Spectra and Crystal Structures of some [1,2,4]Triazolo[1,2-*b*]- and [1,3,4]Thiadiazolo[3,4-*b*]phthalazines

Karoliina Joutsiniemi, Markku Ahlgrén, and Pirjo Vainiotalo*

Department of Chemistry, University of Joensuu, P.O. Box 111, FIN-80101 Joensuu, Finland

Olaf Morgenstern and Mario Meusel

Department of Pharmacy, Ernst-Moritz-Arndt-University,
Ludwig-Jahn-Straße 17, D-17487 Greifswald, Germany
Received September 26, 1994

The mass spectra of ten 1,3-dithioxo[1,2,4]triazolo[1,2-*b*]phthalazines, five 3-iminosubstituted 1-thioxo-[1,3,4]thiadiazolo[3,4-*b*]phthalazines, three 3-iminosubstituted-1-thioxo[1,2,4]triazolo[1,2-*b*]phthalazines, and 1,3-dithioxo-5,10-dihydro[1,3,4]thiadiazolo[3,4-*b*]phthalazine were recorded under electron ionization. The fragmentation pathways were elucidated by metastable ion analysis and exact mass measurements. The changes in the ring-system had little effect on the fragmentation mechanism, but the effect on peak intensities was considerable. The most important fragmentations began with the opening of the triazole ring. Substituents at nitrogen atoms also had a marked effect on the mass spectral behavior. The aryl substituents prompted a whole new fragmentation. The X-ray crystal structure was determined for a few compounds. Two of the three structures of the 1,3-dithioxo[1,2,4]triazolo[1,2-*b*]phthalazines that were studied proved to be relatively planar, whereas the structure of 1,3-dithioxo-5,10-dihydro[1,3,4]thiadiazolo[3,4-*b*]phthalazine was considerably bent similarly to the 2-(4-chlorophenyl)-1,3-dithioxo-2,3,5,10-tetrahydro[1,2,4]triazolo[1,2-*b*]-phthalazine. The triazole and the thiadiazole rings had a strong double bond nature.

J. Heterocyclic Chem., **32**, 283 (1995).

In recent work involving *N,N*-coupled heterobicycles [1-6], we synthesized differently sustituted 1,3-dithioxo-[1,2,4]triazolo[1,2-*b*]phthalazines, **1-10**, 3-iminosubstituted 1-thioxo[1,3,4]thiadiazolo[3,4-*b*]phthalazines, **12-16**, and 3-iminosubstituted 1-thioxo[1,2,4]triazolo[1,2-*b*]-phthalazines, **17-19**, with the purpose of finding new pharmacologically interesting compounds [7,8]. The preparation of compounds **1-10** was achieved either by heating of related 2-thiocarbamoyl-1,2,3,4-tetrahydrophthalazines with carbon disulfide (**3, 6-10**) or by reaction of 1,3-dithioxo-5,10-dihydro[1,3,4]thiadiazolo[3,4-*b*]-phthalazine (**11**) with primary aliphatic amines (**1, 2, 4, 5**). Compound **11** was synthesized by treating 1,2,3,4-tetrahydrophthalazine with carbon disulfide and compounds **12-16** were obtained by treating the differently substituted 2-thiocarbamoyl-1,2,3,4-tetrahydrophthalazines with thiophosgene. The reaction of the 2-thiocarbamoyl-1,2,3,4-tetrahydrophthalazines with arylisothiocyanates under heating yielded compounds **17-19**.

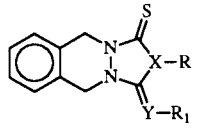

Compound	X	Y	R	R_1
1	N	S	CH_3	—
2	N	S	C_2H_5	—
3	N	S	$CH_2CH{=}CH_2$	—
4	N	S	C_2H_4OH	—
5	N	S	$C_2H_4NC(CH_3)_2$	—
6	N	S	C_6H_5	—
7	N	S	*p*-CH_3-C_6H_4	—
8	N	S	*p*-Cl-C_6H_4	—
9	N	S	naphth-2-yl	—
10	N	S	naphth-1-yl	—
11	S	S	—	—
12	S	N	—	CH_3
13	S	N	—	C_6H_5
14	S	N	—	*p*-Cl-C_6H_4
15	S	N	—	*p*-Br-C_6H_4
16	S	N	—	naphth-2-yl
17	N	N	C_6H_5	C_6H_5
18	N	N	*p*-Cl-C_6H_4	*p*-Cl-C_6H_4
19	N	N	*p*-Br-C_6H_4	*p*-Br-C_6H_4

Mass spectrometry is one of the most useful analytical tools in synthetic chemistry. To obtain maximum benefit from the method it is important to know how different types of compounds behave under mass spectrometric conditions. In this work, the electron ionization mass spectra of compounds **1-19**, listed beside, were recorded and carefully analyzed.

The intention was to find fragmentations that could assist in structural determination of this type of compounds. More specifically, our aim was to determine how this new ring system decomposes in the gas phase under electron ionization and how different substituents affect the fragmentation behavior. Fragmentation pathways were verified by metastable ion analysis and collision induced dissociation technique (CID). Exact mass measurement was used to confirm the elemental composition of the principal fragment ions. The ion structures indicated are nevertheless speculative and merely meant to aid in the visualization of the fragmentation pathways.

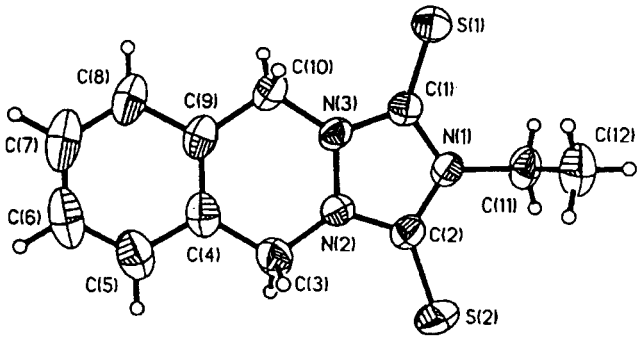

Figure 1. The crystal structure of 2-ethyl-1,3-dithioxo-2,3,5,10-tetrahydro[1,2,4]triazolo[1,2-*b*]phthalazine (**2**).

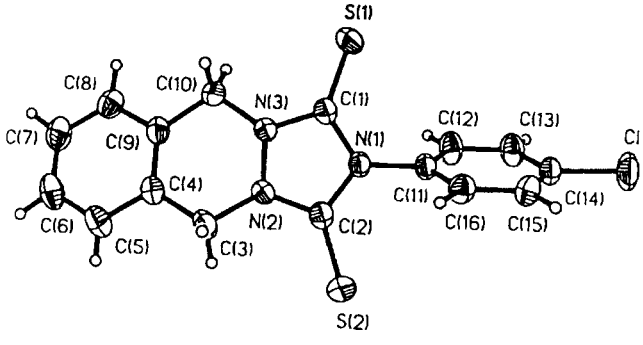

Figure 2. The crystal structure of 1,3-dithioxo-5,10-dihydro[1,3,4]thiadiazolo[3,4-*b*]phthalazine (**8**).

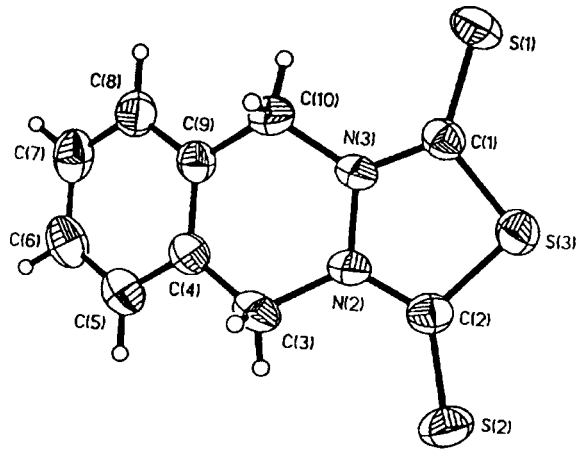

Figure 3. The crystal structure of 2-(4-chlorophenyl)-1,3-dithioxo-2,3,5,10-tetrahydro[1,2,4]triazolo[1,2-*b*]phthalazine (**11**).

Because the connection between the structure and fragmentation was of interest, it was relevant to determine the crystal structure of a few compounds. The X-ray crystal structures were determined for compounds **2**, **4**, **8**, and **11**. The molecular structures of **2**, **8**, and **11** are presented in Figures 1, 2, and 3 respectively. The structure of **4** is isomorphous and isostructural with **2**. As can be seen from the bond lengths and bond angles presented in Tables 1 and 2, the triazole and thiadiazole rings have a strong

Table 1

Bond Lengths for $C_{12}H_{13}N_3S_2$ (**2**), $C_{12}H_{13}N_3OS_2$ (**4**), $C_{16}H_{12}N_3S_2Cl$ (**8**) and $C_{10}H_8N_2S_3$ (**11**)

Compound	**2**	**4**	**8**	**11**	**11**
Molecule				A	B
S(1)-C(1)	1.654(3)	1.664(8)	1.653(2)	1.654(3)	1.653(3)
S(2)-C(2)	1.658(3)	1.659(7)	1.653(2)	1.648(3)	1.647(3)
X-C(1)	1.371(4) [a]	1.365(7) [a]	1.390(3) [a]	1.733(3) [b]	1.740(3) [b]
X-C(2)	1.373(4) [a]	1.375(9) [a]	1.387(3) [a]	1.744(3) [b]	1.744(3) [b]
N(1)-C(11)	1.467(3)	1.482(8)	1.439(3)	—	—
N(2)-N(3)	1.385(4)	1.389(8)	1.391(3)	1.390(3)	1.385(4)
N(2)-C(2)	1.343(3)	1.318(7)	1.346(3)	1.336(4)	1.334(4)
N(2)-C(3)	1.434(4)	1.450(9)	1.459(3)	1.464(4)	1.467(4)
N(3)-C(1)	1.350(4)	1.341(8)	1.346(3)	1.341(4)	1.334(4)
N(3)-C(10)	1.451(3)	1.449(8)	1.450(3)	1.466(4)	1.460(5)
C(3)-C(4)	1.493(4)	1.498(9)	1.500(3)	1.495(5)	1.499(5)
C(4)-C(5)	1.391(5)	1.430(12)	1.392(3)	1.386(5)	1.386(5)
C(4)-C(9)	1.379(5)	1.374(12)	1.378(3)	1.387(4)	1.379(4)
C(5)-C(6)	1.374(5)	1.413(15)	1.386(4)	1.376(5)	1.384(5)
C(6)-C(7)	1.375(7)	1.378(24)	1.374(4)	1.378(5)	1.373(6)
C(7)-C(8)	1.382(6)	1.423(16)	1.379(4)	1.377(5)	1.374(5)
C(8)-C(9)	1.403(4)	1.413(11)	1.400(3)	1.387(5)	1.391(5)
C(9)-C(10)	1.499(5)	1.502(11)	1.510(3)	1.492(5)	1.496(5)
C(11)-C(12)	1.503(6)	1.504(13)	1.380(3)	—	—
O-C(12)	—	1.396(10)	—	—	—
C(12)-C(13)	—	—	1.381(3)	—	—
C(13)-C(14)	—	—	1.382(4)	—	—
C(14)-C(15)	—	—	1.375(4)	—	—
C(15)-C(16)	—	—	1.387(3)	—	—
C(14)-Cl	—	—	1.747(2)	—	—

[a] X = N(1). [b] X = S(3).

Table 2

Bond Angles for $C_{12}H_{13}N_3S_2$ (**2**), $C_{12}H_{13}N_3OS_2$ (**4**), $C_{16}H_{12}N_3S_2Cl$ (**8**), $C_{10}H_8N_2S_3$ (**11**)

Compound Molecule	**2**	**4**	**8**	**11** A	**11** B
C(1)-X-(2)	111.1(2) [a]	110.6(5) [a]	111.6(2) [a]	93.2(1) [b]	92.7(2) [b]
C(1)-N(1)-C(11)	124.3(3)	123.6(6)	124.4(2)	—	—
C(2)-N(1)-C(11)	124.3(2)	125.1(5)	124.0(2)	—	—
N(3)-N(2)-C(2)	108.9(2)	109.6(5)	109.7(2)	115.3(2)	115.7(2)
N(3)-N(2)-C(3)	124.1(2)	123.3(5)	118.9(2)	119.8(2)	119.8(2)
C(2)-N(2)-C(3)	126.6(3)	126.4(6)	127.2(2)	124.8(2)	124.3(3)
N(2)-N(3)-C(1)	109.2(2)	108.4(5)	109.5(2)	114.9(2)	114.7(3)
N(2)-N(3)-C(10)	122.8(2)	122.7(5)	121.8(2)	119.9(2)	119.8(3)
C(1)-N(3)-C(10)	126.4(3)	127.2(6)	125.7(2)	125.1(2)	125.5(3)
S(1)-C(1)-X	127.8(2) [a]	127.9(5) [a]	129.2(1) [a]	124.7(2) [b]	124.8(2) [b]
S(1)-C(1)-N(3)	127.0(2)	126.5(5)	126.2(2)	126.8(2)	126.5(3)
X-C(1)-N(3)	105.1(3) [a]	105.6(6) [a]	104.5(2) [a]	108.5(2) [b]	108 8(2) [b]
S(2)-C(2)-X	127.9(2) [a]	127.1(4) [a]	128.6(2) [a]	124.2(2) [b]	124.9(2) [b]
S(2)-C(2)-N(2)	126.5(3)	127.2(6)	126.9(2)	127.7(2)	127.0(2)
X-C(2)-N(2)	105.6(2)	105.7(6)	104.5(2)	108.1(2)	108.1(2)
N(2)-C(3)-C(4)	112.8(3)	112.4(6)	110.2(2)	111.7(2)	110.8(2)
C(3)-C(4)-C(5)	118.5(3)	115.8(8)	119.5(2)	120.5(3)	120.5(3)
C(3)-C(4)-C(9)	122.2(3)	122.8(7)	120.9(2)	119.3(3)	119.0(3)
C(5)-C(4)-C(9)	119.3(3)	121.4(7)	119.6(2)	120.1(3)	120.5(3)
C(4)-C(5)-C(6)	120.9(4)	119.1(11)	120.8(3)	120.1(3)	119.0(3)
C(5)-C(6)-C(7)	119.9(4)	117.6(11)	119.5(2)	119.7(3)	121.0(4)
C(6)-C(7)-C(8)	120.3(3)	124.7(11)	120.3(2)	120.7(3)	119.8(3)
C(7)-C(8)-C(9)	119.7(4)	116.2(10)	120.4(2)	119.9(3)	120.2(3)
C(4)-C(9)-C(8)	119.9(3)	120.9(7)	119.3(2)	119.5(3)	119.5(3)
C(1)-C(9)-C(10)	122.3(3)	121.5(6)	122.5(2)	119.3(3)	119.3(3)
C(8)-C(9)-C(10)	117.8(3)	117.7(7)	118.1(2)	121.3(3)	121.1(3)
N(3)-C(10)-C(9)	112.0(3)	112.7(6)	112.3(2)	111.4(3)	111.2(3)
N(1)-C(11)-C(12)	111.5(2)	107.4(5)	119.1(2)	—	—
O-C(12)-C(11)	—	108.5(7)	—	—	
N(1)-C(11)-C(16)	—	—	119.4(2)	—	—
C(12)-C(11)-C(16)	—	—	121.5(2)	—	—
C(11)-C(12)-C(13)	—	—	119.7(2)	—	—
C(12)-C(13)-C(14)	—	—	118.7(2)	—	—
C(13)-C(14)-C(15)	—	—	121.9(2)	—	—
C(14)-C(15)-C(16)	—	—	119.3(2)	—	—
C(11)-C(16)-C(15)	—	—	118.8(2)	—	—

[a] X = N(1). [b] X = S(3).

double-bond nature due to the resonance effects between the thioxo substituent and the triazole/thiadiazole moiety. With **2** and **4** the molecules are nearly planar, the angle between the triazole and phenylene rings being 5.0° and 6.1°, respectively. With **11** the two independent molecules (A and B) are equal (Tables 1 and 2), but similarly to compound **8** the molecules are not planar and the thiadiazole and phenylene rings form the angles of 32.1° and 33.4° in molecules A and B, respectively, the corresponding angle being 22.8° in **8**. The N(1)-C(11) bond length of 1.439(3) Å in **8** is somewhat shorter than in **2** (1.467(3) Å) and **4** (1.482(8) Å) due to the aromaticy of the *N*-substituent. The phenyl ring does not, however, take place in the π-bonding in the triazole ring, the torsion angle of C(12)-C(11)-N(1)-C(1) being -67.2(3)°.

On the basis of the mass spectrometric behavior the 19 compounds examined can be divided into two groups: 1,3-dithioxo compounds, **1-11**, and 1-imino-3-thioxo compounds, **12-19**. The 70 eV electron ionization mass spectra of the compounds are presented in Table 3 and in Figures 4 and 5. The spectra show that the molecular ion peak is very intense in every spectrum; often it is the base peak.

In principle, compounds **1-10** behaved in the same way even though the substituents had some influence on the decompositions. There were two important primary fragmentations which began with the opening of the triazole ring. One was the loss of RNHCS, which led to the formation of the $[C_9H_7N_2S]^+$ ion at m/z 175. The other fragmentation led to the formation of the $[C_8H_7N]^{+\bullet}$ ion at m/z 117. The loss of $HS^\bullet$ might also be described as a primary fragmentation from the molecular ion. The $[M\text{-}HS]^+$ ion so formed decomposed further to the $[C_9H_7N_2]^+$ ion at m/z 143. Additional primary fragmentations gave rise to the ions $[C_8H_8N]^+$ and $[C_8H_8]^{+\bullet}$ at m/z 118 and m/z 104, respectively. The m/z 104 ion represents a retro-Diels-Alder (RDA) fragmentation which, according to the

peak intensity, seemed to be important in the decomposition of compounds **1-10** (Figure 4, Table 3). The fact that the RDA reaction took place suggests that with the molecular ions, in spite of several heteroatoms, the charge

Table 3

Principal Fragment Ions (Intensity ≥ 5) in the Mass Spectra of the Compouds **2**, **3** and **5-19**. Data are Corrected for ^{37}Cl and ^{81}Br Contributions, Otherwise Uncorrected, m/z (% Relative Intensities)

Compound	m/z (relative intensity)
2	2-Ethyl-1,3-dithioxo-2,3,5,10-tetrahydro[1,2,4]triazolo[1,2-*b*]phthalazine 265 (10), 264 (17), 263 (100) $M^{+\cdot}$, 262 (12), 234 (7), 230 (9), 175 (10), 143 (12), 118 (34), 117 (53), 116 (16), 113 (9), 105 (8), 104 (27), 103 (14), 102 (11), 91 (7), 90 (8), 89 (8), 88 (5), 78 (10), 77 (8), 60 (7)
3	2-Allyl-1,3-dithioxo-2,3,5,10-tetrahydro[1,2,4]triazolo[1,2-*b*]phthalazine 277 (10), 276 (18), 275 (100) $M^{+\cdot}$, 274 (5), 242 (22), 217 (7), 201 (6), 175 (30), 162 (15), 143 (12), 137 (6), 135 (8), 118 (29), 117 (32), 116 (28), 105 (21), 104 (40), 103 (18), 102 (24), 99 (8), 91 (9), 90 (8), 89 (9), 78 (14), 77 (11), 41 (14), 39 (11)
5	2-(2-Isopropylidenaminoethyl)-1,3-dithioxo-2,3,5,10-tetrahydro[1,2,4]triazolo[1,2-*b*]phthalazine 320 (5), 319 (10), 318 (49) $M^{+\cdot}$, 237 (13), 236 (41), 235 (100), 734 (40), 175 (14), 159 (6), 143 (9), 135 (7), 118 (32), 117 (32), 116 (13), 104 (18), 103 (17), 102 (9), 91 (9), 90 (6), 89 (6), 84 (26), 83 (17), 78 (9), 77 (8), 70 (19), 68 (12), 42 (12), 41 (7), 30 (8)
6	2-Phenyl-1,3-dithioxo-2,3,5,10-tetrahydro[1,2,4]triazolo[1,2-*b*]phthalazine 313 (11), 312 (21), 311 (99) $M^{+\cdot}$, 310 (12), 278 (9), 219 (6), 175 (11), 161 (20), 156 (6), 143 (17), 136 (18), 135 (37), 118 (20), 117 (100), 116 (15), 105 (7), 104 (25), 103 (15), 91 (8), 90 (9), 89 (7), 78 (14), 77 (28), 51 (10)
7	2-(4-Methylphenyl)-1,3-dithioxo-2,3,5,10-tetrahydro[1,2,4]triazolo[1,2-*b*]phthalazine 327 (11), 326 (22), 325 (98) $M^{+\cdot}$, 324 (16), 292 (10), 176 (6), 175 (35), 163 (8), 150 (19), 149 (39), 143 (19), 135 (8), 132 (5), 131 (6), 118 (25), 117 (100), 116 (17), 105 (7), 104 (25), 103 (14), 92 (10), 91 (36), 90 (10), 89 (10), 78 (13), 77 (11), 65 (11), 63 (5), 51 (5), 39 (7)
8	2-(4-Chlorophenyl)-1,3-dithioxo-2,3,5,10-tetrahydro[1,2,4]triazolo[1,2-*b*]phthalazine 346/348 (30), 345/347 (68) $M^{+\cdot}$, 344 (11), 312 (6), 195/197 (12), 175 (11), 173 (6), 170/172 (10), 169/171 (26), 143 (20), 135 (6), 118 (18), 117 (100), 116 (15), 111 (8), 105 (7), 104 (26), 103 (14), 91 (10), 90 (10), 89 (7), 78 (11), 77 (8), 75 (6)
9	2-(Naphth-2-yl)-1,3-dithioxo-2,3,5,10-tetrahydro[1,2,4]triazolo[1,2-*b*]phthalazine 363 (12), 362 (25), 361 (100) $M^{+\cdot}$, 360 (11), 328 (8), 269 (6), 211 (14), 187 (5), 186 (20), 185 (74), 181 (8), 175 (16), 164 (8), 153 (8), 151 (5), 143 (19), 135 (15), 131 (8), 128 (11), 127 (27), 118 (36), 117 (63), 116 (13), 115 (8), 105 (5), 104 (23), 103 (13), 91 (7), 90 (7), 89 (6), 78 (11), 77 (10)
10	2-(Naphth-1-yl)-1,3-dithioxo-2,3,5,10-tetrahydro[1,2,4]triazolo[1,2-*b*]phthalazine 363 (12), 362 (26), 361 (100) $M^{+\cdot}$, 360 (14), 328 (8), 269 (6), 233 (7), 211 (14), 186 (16), 185 (62), 181 (9), 175 (22), 153 (9), 143 (18), 135 (12), 131 (27), 130 (7), 128 (19), 127 (19), 118 (27), 117 (65), 116 (13), 115 (7), 104 (21), 103 (14), 91 (7), 90 (6), 89 (6), 78 (10), 77 (11), 76 (9), 51 (5)
11	1,3-Dithioxo-5,10-dihydro[1,3,4]thiadiazolo[3,4-*b*]phthalazine 254 (14), 253 (14), 252 (95) $M^{+\cdot}$, 193 (12), 175 (18), 161 (6), 143 (11), 136 (7), 135 (14), 118 (15), 117 (100), 116 (10), 104 (29), 103 (19), 102 (22), 91 (9), 90 (10), 89 (9), 78 (15), 77 (13), 76 (5), 74 (7), 63 (7), 52 (7), 51 (11), 39 (8)
12	3-Methylimino-1-thioxo-5,10-dihydro[1,3,4]thiadiazolo[3,4-*b*]phthalazine 251 (10), 250 (15), 249 (100) $M^{+\cdot}$, 177 (8), 176 (29), 175 (85), 149 (11), 143 (6), 118 (14), 117 (65), 115 (14), 104 (35), 103 (18), 91 (13), 90 (9), 89 (10), 78 (15), 77 (12), 63 (6), 39 (7)
13	3-Phenylimino-1-thioxo-5,10-dihydro[1,3,4]thiadiazolo[3,4-*b*]phthalazine 313 (11), 312 (20), 311 (100) $M^{+\cdot}$, 193 (6), 177 (7), 176 (29), 175 (82), 149 (8), 136 (9), 135 (39), 118 (18), 117 (68), 116 (11), 104 (49), 103 (23), 91 (14), 90 (9), 89 (8), 78 (19), 77 (24), 65 (6), 63 (5), 51 (12), 39 (7)
14	3-(4-Chlorophenyl)imino-1-thioxo-5,10-dihydro[1,3,4]thiadiazolo[3,4-*b*]phthalazine 346/348 (21), 345/347 (100) $M^{+\cdot}$, 193 (6), 177 (8), 176 (34), 175 (95), 171 (15), 170 (6), 169 (41), 149 (11), 143 (9), 136 (6), 135 (9), 131 (8), 118 (23), 117 (97), 116 (16), 111 (9), 105 (7), 104 (58), 103 (27), 102 (8), 91 (16), 90 (14), 89 (11), 78 (23), 77 (15), 75 (10), 65 (5), 63 (8), 56 (5), 51 (9), 50 (5), 39 (8)
15	3-(4-Bromophenyl)imino-1-thioxo-5,10-dihydro[1,3,4]thiadiazolo[3,4-*b*]phthalazine 393 (8), 390/392 (14), 389/391 (67) $M^{+\cdot}$, 213/215 (25), 193 (10), 177 (8), 176 (37), 175 (100), 155 (9), 149 (10), 143 (7), 136 (6), 135 (9), 134 (5), 118 (23), 117 (96), 116 (16), 105 (5), 104 (57), 103 (27), 102 (12), 91 (15), 90 (14), 89 (10), 78 (22), 77 (14), 76 (8), 75 (8), 63 (8), 51 (8), 50 (6), 39 (7)
16	3-(Naphth-2-yl)imino-1-thioxo-5,10-dihydro[1,3,4]thiadiazolo[3,4-*b*]phthalazine 363 (12), 362 (25), 361 (100) $M^{+\cdot}$, 345 (6), 193 (6), 186 (9), 185 (38), 180 (6), 177 (5), 176 (22), 175 (66), 168 (6), 167 (7), 153 (8), 149 (7), 143 (5), 135 (5), 128 (6), 127 (14), 126 (5), 118 (20), 117 (66), 116 (10), 115 (10), 104 (40), 103 (16), 91 (9), 90 (6), 89 (6), 78 (14), 77 (10)
17	2-Phenyl-3-phenylimino-1-thioxo-2,3,5,10-tetrahydro[1,2,4]triazolo[1,2-*b*]phthalazine 372 (8), 371 (27), 370 (100) $M^{+\cdot}$, 369 (25), 278 (6), 234 (5), 220 (8), 219 (8), 195 (9), 194 (30), 175 (5), 136 (8), 135 (33), 118 (21), 117 (49), 116 (7), 104 (32), 103 (13), 91 (10), 90 (6), 78 (12), 77 (26), 51 (8)
18	2-(4-Chlorophenyl)-3-(4-chlorophenyl)imino-1-thioxo-2,3,5,10-tetrahydro-[1,2,4]triazolo[1,2-*b*]phthalazine 441 (14), 439 (28), 438/440/442 (71) $M^{+\cdot}$, 437 (14), 262/264 (18), 175 (8), 171 (31), 170 (13), 169 (82), 152 (6) 143 (7), 135 (9), 134 (38), 133 (21), 132 (8), 131 (10), 127 (6), 119 (6), 118 (59), 117 (82), 116 (21), 111/113 (33), 105 (18), 104 (100), 103 (26), 102 (6), 91 (14), 90 (15), 89 (10), 78 (23), 77 (15), 76 (7), 75 (23), 63 (8), 51 (11), 50 (10), 39 (7)
19	2-(4-Bromophenyl)-3-(4-bromophenyl)imino-1-thioxo-2,3,5,10-tetahydro[1,2,4]triazolo[1,2-*b*]phthalazine 531 (14), 529 (35), 527 (30), 526/528/530 (100) $M^{+\cdot}$, 525 (9), 350/352/354 (20), 225 (7), 224 (7), 219 (8), 213/215 (22), 175 (8), 155/157 (7), 143 (9), 135 (13), 134 (8), 132 (6), 118 (32), 117 (86), 116 (17), 105 (14), 104 (92), 103 (29), 102 (9), 91 (16), 90 (24), 89 (10), 78 (24), 77 (12), 76 (12), 75 (10), 63 (9), 51 (5), 50 (5), 39 (6)

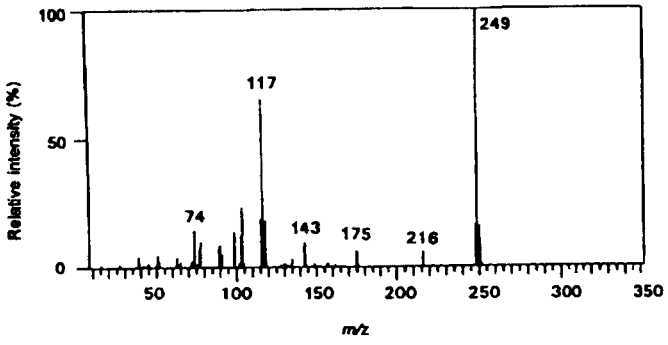

Figure 4. The 70 eV mass spectrum of 2-methyl-1,3-dithioxo-2,3,5,10-tetrahydro[1,2,4]triazolo[1,2-*b*]phthalazine (**1**).

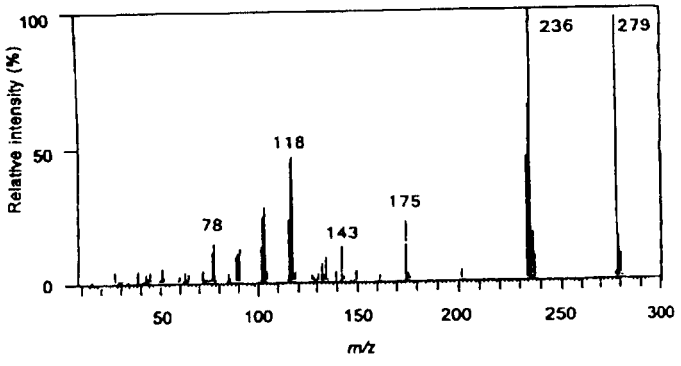

Figure 5. The 70 eV mass spectrum of 2-(2-hydroxyethyl-1,3-dithioxo-2,3,5,10-tetrahydro[1,2,4]triazolo[1,2-*b*]phthalazine (**4**).

was partially located at the benzene ring. It is also noteworthy that in this reaction the charge remained only with the hydrocarbon part ($[C_8H_8]^{+\bullet}$ at m/z 104) of the molecule. As an example, the principal fragmentations of compound **1** are presented in Scheme 1.

Scheme 1

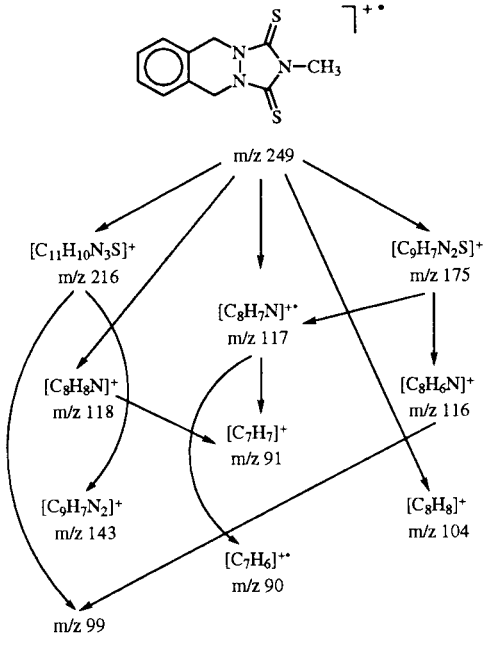

The most important fragmentations of the ring system began with the opening of the triazole ring. This is somewhat surprising because, according to the crystallographic studies, the triazole ring should be stabilized by resonance, in contrast to the pyridazine ring. The formation of the $[C_9H_7N_2S]^+$ ion at m/z 175 may be rationalized as decribed in Scheme 2: the triazole ring decomposes by breaking of the bond between the 1-carbon and 2-nitrogen with a simultaneous migration of one hydrogen atom to the leaving group.

Scheme 2

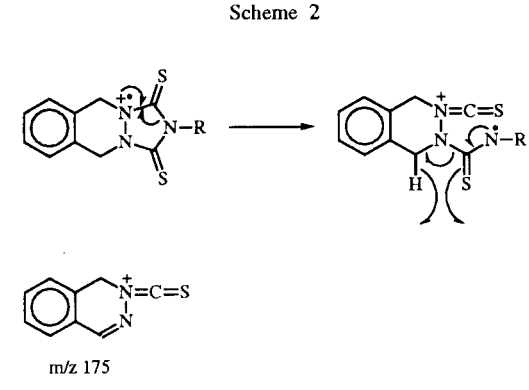

According to the metastable ion studies the $[C_8H_7N]^{+\bullet}$ ion at m/z 117 was formed directly from the molecular ion. In some cases it could have been formed *via* the m/z 175 ion even though this requires the formation of the radical cation from the cation. This can be explained in terms of the stability of the m/z 117 ion, which is reflected in its large peak intensity in every spectrum of compounds **1-10**. With compounds **6-8** the $[C_8H_7N]^{+\bullet}$ ion at m/z 117 represented the base peak in the spectrum. The formation of the $[C_8H_7N]^{+\bullet}$ ion evidently began with a radical-site initiated cleavage with respect to the nitrogen atom at position four (Scheme 3).

Scheme 3

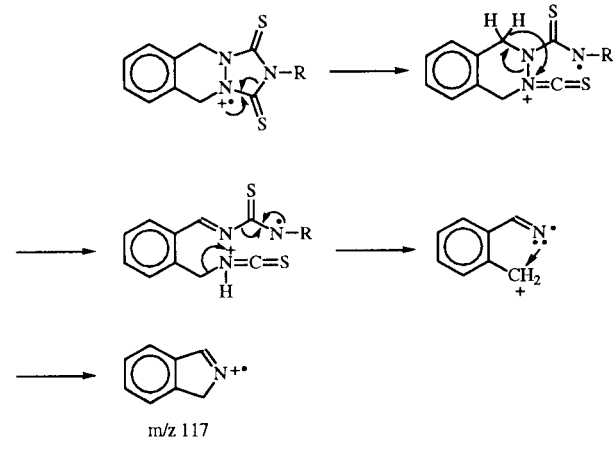

This cleavage was followed by the migration of a hydrogen atom most probably from the 10-carbon to the 4-nitrogen leading to the ring-opening. Next the loss of SCNR through another radical-site initiated cleavage with respect to the 2-nitrogen and the inductive cleavage of HNCS took place, giving rise to the $[C_8H_7N]^{+\bullet}$ ion at m/z 117. The last two reactions had to occur simultaneously, or at least very close together, because neither of the cleavages could be observed separately, either in the ion source or in the metastable time frame. The ion $[C_8H_7N]^{+\bullet}$ at m/z 117 decomposed further giving rise to the ions $[C_7H_6]^{+\bullet}$ and $[C_7H_7]^{+\bullet}$ at m/z 90 and m/z 91, respectively. The ion $[C_8H_8N]^+$ at m/z 118 must be formed in a corresponding way to the m/z 117 ion but without the hydrogen rearrangement.

The nature of the substituent R at the 2-nitrogen had a marked effect on the fragmentation behavior of the compounds. All alkyl substituents except methyl group prompted new fragmentations, though the effect of the ethyl group was minor, causing only the elimination of $C_2H_5^{\bullet}$. Increase in the size of the substituent and/or the existence of a functional group had a marked effect on the fragmentations. With compounds **3-5** the effect of the substituent was clearly evident as the decreased importance of the $[C_8H_7N]^{+\bullet}$ ion at m/z 117 and increased importance of the $[C_8H_8N]^+$ ion at m/z 118. With compounds **4** and **5** the loss of the substituent was the most important reaction. The substituent was eliminated as such through a simple bond cleavage or through migration of one or two hydrogen atoms from the substituent to the ring system. The migration of one hydrogen to the nitrogen with simultaneous breaking of the N-C bond is a typical reaction for nitrogen compounds [9]. With compound **5** this reaction led to the base peak of the spectrum at m/z 235. With compound **4**, on the other hand, a fragmentation demanding a rearrangement of two hydrogens led to the base peak of the spectrum, at m/z 236 (Figure 5).

The replacement of the alkyl group with an aromatic substituent at the 2-nitrogen in compounds **6-10** seemed to increase the importance of the ion at m/z 117 at least compared with compounds **3-5**. There was also a new primary fragmentation with compounds **6-10** which led to the formation of the $[RNCS]^+$ ion. No corresponding fragmentation was found in the spectra of compounds **1-5**. The formation of the ion $[RNCS]^+$ indicates, that in the ionization process, an electron was partly removed from the π-electron system of the aryl substituent. This effect was particularly evident with the naphthyl substituted compounds **9** and **10**. An electron withdrawing chlorine substituent in the phenyl ring (compound **8**) tended to suppress this reaction.

As mentioned above the replacement of the 2-nitrogen with a sulfur atom bent the ring system considerably, but it did not have a noticeable effect on the fragmentation pattern. This can be seen by comparing the spectra of compounds **1** and **11**, which were in principle similar; only the relative peak intensities differed.

The replacement of the sulfur atom at position one or three in the 1,3-dithioxo[1,3,4]-thiadiazolo system with an N-R group (compounds **12-16**) likewise effected little change in the fragmentation pathways, but it had a considerable effect on peak intensities (Table 3). The primary fragmentations led to the formation of ions at m/z 176, m/z 175, m/z 118, m/z 117, and m/z 104. As with compounds **1-11** the two most important fragmentations in compounds **12-16** began with the opening of the triazole ring leading to the formation of the ions m/z 175 and m/z 117. It is noteworthy that the ion m/z 175 was now strikingly intense, giving rise to the most abundant fragment ion peak of the spectra. The formation mechanism of the ion m/z 175 was most probably the same with compounds **12-16** as with compounds **1-11** (Scheme 2): the triazole ring decomposed by breaking of the bond between the 1-carbon and 2-sulfur with a coexistent migration of one hydrogen atom to the eliminated group. The presence of a nitrogen atom at the 3-carbon, and not sulfur as in compounds **1-11**, probably was the reason for the strong intensity of the ion at m/z 175. As a stronger nucleophile than sulfur, the nitrogen may encourage the migration of the hydrogen.

The fragmentation mechanism leading to the formation of the m/z 117 ion was analogous to that observed for compounds **1-11** except in the final stage of the mechanism the elimination of the SCNR and HNCS groups was not simultaneous but successive. For this reason the m/z 176 ion corresponding to the elimination of the SCNR group was relatively abundant.

In compounds **17-19** the sulfur atom in one of the thioxo groups in the 1,3-dithioxo[1,2,4]triazolo system is replaced with an N-R group. In the spectra, the peak intensities differed considerably from those observed for compounds **1-11** and also for compounds **12-16**, but the replacement seemed to have little effect on the fragmentation mechanisms. The primary fragmentations leading to the formation of the ions at m/z 175, m/z 118, m/z 117, and m/z 104 in compounds **12-16** were also observed for compounds **17-19**. However, the intensity of the ion m/z 175 was a great deal less for compounds **17-19** than compounds **12-16**, even though the formation mechanism was probably the same.

As noted above, the removal of an electron from the aryl substituent at position two most probably caused the formation of the ion $[RNCS]^+$ in compounds **6-10**. The same reaction took place in compounds **13-19**. Since compounds **17-19** have two phenyl substituents, either one of them could have started the fragmentation leading to the $[RR_1CN_2]^{+\bullet}$ and $[RNCS]^+$ ions. The formation of these particular ions demands that in the ionization

Table 4

Crystallographic Data for **2**, **4**, **8**, and **11**

Compound	**2**	**4**	**8**	**11**
Formula	$C_{12}H_{13}N_3S_2$	$C_{12}H_{13}N_3OS_2$	$C_{16}H_{12}N_3S_2Cl$	$C_{10}H_8N_2S_3$
Fw	263.4	279.4	345.9	252.4
Crystal system	Monoclinic	Monoclinic	Monoclinic	Monoclinic
Space group	C2/c	C2/c	$P2_1/c$	$P2_1/c$
a/Å	23.460(3)	24.132(5)	11.243(3)	10.762(3)
b/Å	12.869(2)	13.039(2)	19.242(3)	12.269(4)
c/Å	9.054(2)	9.001(10)	7.136(2)	16.689(4)
β/°	111.62(2)	111.62(10)	93.34(2)	95.13(2)
U/Å^3	2541.2(4)	2633.2(7)	1541.2(6)	2194.8(11)
Z	8	8	4	8
D_c/gcm^{-3}	1.377	1.409	1.491	1.527
F(000)	1104	1168	712	1040
2θ range °	5-114	4-55	4-60	5-55
Radiation	Cu-Kα	Mo-Kα	Mo-Kα	Mo-Kα
No. of unique refl.	1714	3041	4508	5062
Obs. data [I≥2σ(I)]	1412	1682	2928	3143
μ/mm^{-1}	3.635	0.379	0.504	0.615
No. of parameters	154	163	247	271
R[a]	0.047	0.096	0.044	0.042
wR[b]	0.053	0.158	0.049	0.078
w	$1/\{\sigma^2(F)+0.002F^2\}$	$1/\{\sigma^2(F)+0.001F^2\}$	$1/\{\sigma^2(F)+0.005F^2\}$	$1/\{\sigma^2(F)+0.001F^2\}$
Goodness of fit[c]	1.51	2.22	1.30	1.07

[a] $R = (\Sigma|\,|F_0|-|F_c|\,|)/\Sigma|F_0|$. [b] $wR = [\Sigma w(|F_0|-|F_c|)^2/\Sigma w(|F_0|)^2]^{1/2}$, where $w^{-1} = [\sigma^2(F)+gF^2]$. [c] Goodness of fit $= [\Sigma w(|F_0|-|F_c|)^2/(N_0-N_v)]^{1/2}$ where N_0 = No. of obs. ref., N_v = No. of varables, $w^{-1} = [\sigma^2(F)+gF^2]$.

process an electron was removed from the π-electron system of the aryl substituent and hence they are seen only in the spectra of aryl substituted compounds.

The RDA reaction product, the m/z 104 ion, was particularly abundant for compounds **18** and **19**; with **18** the ion m/z 104 represented the base peak in the spectrum and with **19** it was the most abundant fragment ion. This means that the electronegative halogen atoms at the *para*-position of the substituents R and R_1 affect the electron density in the molecule so that an electron can be removed from the benzene ring in the ring system especially easily.

The $[M-HS]^+$ ion peak was considerably smaller for compounds **12-19** than for compounds **1-11** and sometimes did not appear in the spectrum at all. The elimination of HS$^\bullet$ nevertheless occured with all the compounds: for the metastable ion studies showed that the m/z 143 ions, which were always present, were formed *via* the $[M-HS]^+$ ions.

EXPERIMENTAL

X-ray Crystallographic Analyses of **2**, **4**, **8**, and **11**.

Synthesis and spectroscopic characterization of the compounds have been presented elsewhere [7,8]. Crystals of **2** and **11** used for the X-ray crystal structural analyses were obtained from acetone, crystals of **4** from acetone/methanol and crystals of **8** from toluene/1-butanol. Data were collected on a Siemens R3m diffractometer using Mo-Kα radiation (λ = 0.71073) for **4**, **8**, and **11** and Cu-Kα radiation (λ = 1.54278) for **2**, and using ω-scan mode with scan widths 0.50° (**2**), 0.70° (**4**), 0.9° (**8**), and 0.80° (**11**) from $K\alpha_{1,2}$ and variable scan speeds of 2.00-29.3 min^{-1} (**2**), 2.49-29.3 min^{-1} (**4**, **11**), and 2.93-29.3 min^{-1} (**8**).

Accurate cell parameters were obtained from 25 automatically centered reflections, in the range $15° < 2\theta < 25°$. Other crystallographic data are presented in Table 4. The structures were solved by direct methods and subsequent Fourier synthesis. No hydrogen atoms were refined anisotropically. Hydrogen atoms were placed at calculated positions in **2**, **4**, and **11** with fixed isotropic thermal parameters (C-H = 0.96 Å and U = 0.08 Å^2) except the hydroxyl hydrogen atom in **4**, which was located from a difference Fourier map and was not refined. In **8** the hydrogen atoms were located from difference maps and refined isotropically, the C-H bond lengths varying from 0.88(3) Å to 1.01(3) Å and the isotropic temperature factors from 0.034(6) to 0.082(11) Å^2. The SHELXTL PLUS program package was used for all calculations [10].

Mass spectrometric measurements were made on a Jeol JMS-D300 mass spectrometer equipped with a JMA-2000H data system. Samples were introduced through a direct inlet probe at temperatures 110-250°. Typical source conditions were: temperature 170°, electron energy 70 eV, accelerating voltage 3 keV, and ionization current 300 μA. The CID mass spectra were measured by using linked scans at constant B/E with helium led into the first field-free region so that the transmission of the main beam was 33%. Accurate mass measurements were carried out at a nominal resolving power of 5000. Perfluorokerosine (PFK) was used as reference compound.

Supplementary Materials.

Tables of observed and calculated structure factors, atomic coordinates, and anisotropic temperature factors are available from the authors.

REFERENCES AND NOTES

* Author to whom correspondence should be addressed.

[1] O. Morgenstern, P. H. Richter, and A. Klemann, *Pharmazie*, **46**, 418 (1991).

[2] O. Morgenstern, A. Klemann, and P. H. Richter, *Pharmazie*, **46**, 505 (1991).

[3] A. Klemann, O. Morgenstern, and P. H. Richter, *Pharmazie*, **46**, 573 (1991).

[4] A. Klemann, O. Morgenstern, and P. H. Richter, *Pharmazie*, **46**, 637 (1991).

[5] O. Morgenstern, A. Klemann, and P. H. Richter, *Pharmazie*, **46**, 416 (1991).

[6] O. Morgenstern, M. Ahlgrén, J. Vepsäläinen, P. H. Richter, and P. Vainiotalo, *J. Chem. Soc., Perkin Trans. 2*, in press.

[7] O. Morgenstern, M. Meusel, and P. H. Richter, *Pharmazie*, **49**, 489 (1994).

[8] O. Morgenstern, M. Meusel, S. Denke, J. Vepsäläinen, and P. H. Richter, *Pharmazie*, **49**, 419 (1994).

[9] A. J. Blackman and J. H. Bovvie, *Org. Mass Spectrom.*, **7**, 57 (1973).

[10] SHELXTL PLUS, Release 4.11/V, Siemens Analytical X-ray Instruments Inc, Madison, Wisconsin, 1990.